Temperature- and saturation-dependent behaviour of unsaturated clay beams in bending tests

Maximilian Hardenberg[1*] and *Christos* Vrettos[1]

[1]Division of Soil Mechanics and Foundation Engineering, Technical University of Kaiserslautern, Kaiserslautern, Germany

Abstract. The paper investigates the deformation behaviour of partially saturated clay beams under flexural stress. Beams were prepared from two clays and then loaded until failure. Three degrees of saturation and two loading rates were examined for each clay. The load, the matric suction at different beam points, and deflection in the middle of the beam were measured during the tests. The loading device ensures an even distribution of stresses on the top surface of the beam, which was confirmed by employing tactile pressure matrix sensors placed between the loading device and the beam. In addition to the tests at room temperature, tests at 55 °C were carried out in a walk-in climate chamber to assess the effects of temperature. The paper summarises the testing procedure and presents selected experimental results.

1 Introduction

A key integrity criterion of mineral landfill sealings is their deformation capacity when subjected to uneven mechanical loading. Since the composition of the landfill body is inhomogeneous, it is impossible to prevent bending stresses in the sealing due to differential deformations. If these stresses exceed the tensile strength, they can lead to cracks in the sealing, significantly affecting their functionality [1].

The issue of deformation capacity arose in recent years in Germany in connection with the innovative and sustainable concept of 'landfill-on-landfill', as shown in Fig. 1. Hence, the deformation capacity of mineral sealings inevitably advanced to a significant issue in the design of such structures.

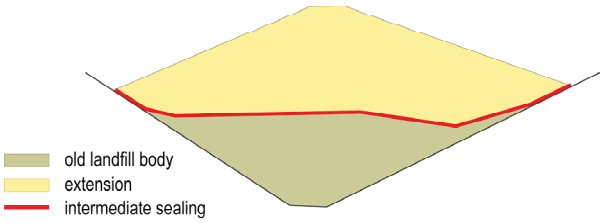

Fig. 1. Schematic illustration of the 'landfill-on-landfill' concept [1].

For fine-grained soils, verification of sufficient deformation capacity is one of the main criteria when assessing their suitability for mineral sealing. The acceptance of an induced deformation is verified via the tensile strength and maximum allowable tensile strain. In compacted fine-grained soils, the tensile strength, which governs the risk of cracking and crack propagation, is mainly due to soil suction. The total soil suction consists of two components, the matric and osmotic suction which are controlled by chemical and physical bonding forces [2]. The tensile strength, also depending on the clay type and content, density and degree of saturation is closely connected to the soil suction.

In the frame of a research project, the deformation capacity of various clays has been assessed by utilising appropriate bending tests at different degrees of saturation, ambient temperatures and loading rates. Findings from the first test series are presented in the following.

2 Tensile strength of unsaturated clays

Direct and indirect methods are available to determine the tensile strength of unsaturated cohesive soils. In direct methods, the tensile stress is directly applied on the specimen. The tensile strength can be directly determined from the uniform stress distribution which is generated over the cross-section. Methods commonly used are tensile tests on hollow cylinders [3] or the so-called 8-shaped specimen [4, 5].

Commonly used indirect methods are bending tests [1, 6–9], uniaxial compression tests [4], and splitting tensile tests [10]. Bending tests are usually carried out as 3-point or 4- point bending tests, but other setups are also possible [1]. The bending test results presented in [6, 7, 9] show that the stress distribution over the beam cross-section is non-linear rather than linear. This requires particular attention in evaluating tensile strength. Three options for deriving the tensile strength from bending tests are described in [11].

* Corresponding author: maximilian.hardenberg@bauing.uni-kl.de

3 Soil properties and specimen preparation

Before the bending tests could be carried out, four suitable clays were selected based on soil classification tests. Results only for two of them are presented herein. After the materials were selected, three water contents were defined with which the beams were produced and subsequently tested.

The first clay is an inorganic kaolinite of high plasticity, referred to as GD, and the second is an inorganic kaolinite of medium plasticity, referred to as TK. The respective grain size distribution curves are displayed in Fig. 2.

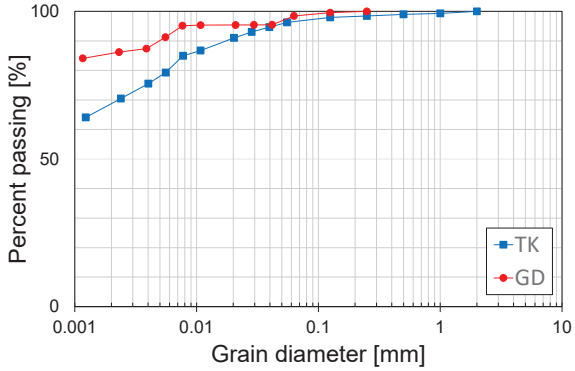

Fig. 2. Grain size distribution curves.

The relevant soil mechanical parameters are summarised in Table 1 with d_{50} denoting the median grain size, w_L the water content at the liquid limit state, I_P the plasticity index, ρ_{Pr} the proctor density, w_{Pr} the water content corresponding to the proctor density and w_A the water absorption capacity.

Table 1. Soil properties of the investigated clays.

	GD	TK
d_{50} [mm]	< 0.001	< 0.001
w_L [%]	59.3	40.6
I_P [%]	33.1	20.8
w_{Pr} [%]	26.3	18.8
ρ_{Pr} [t/m³]	1.42	1.67
w_A [%]	76.1	67.9

Both clays were tested at relative Proctor density D_{Pr} = 100 % and D_{Pr} = 97 % on the 'dry' and the 'wet' side, respectively. These values correspond to water contents or consistencies I_C, as summarised in Table 2. It can be seen that both GD and TK move with increasing water content from a 'very stiff' state ($I_C > 1.0$) to a 'stiff' state ($0.75 < I_C < 1.0$), cf. EN ISO 14688-2:2018.

Table 2. Consistency index I_C at different Proctor densities.

	I_C [-]	
	GD	TK
D_{Pr} = 97 % 'dry side'	1.01	1.16
D_{Pr} = 100 %	0.89	1.05
D_{Pr} = 97 % 'wet side'	0.75	0.93

To facilitate clay beam preparation with the placement of clays in prismatic steel moulds, clay was first shredded, and the amount of water to achieve the desired water content was added. The material was mixed well and left to rest for a day at room temperature before being placed.

The clay beams were prepared in prismatic steel moulds with length/height/width equal to 778/100/100 mm. All sides of the steel mould were cleaned, lubricated and lined with a thin layer of paper to facilitate the later removal of the beam. The total amount of material for each beam was divided into six parts, placed in the mould, and compacted in layers. After compaction, their surfaces were roughened again to ensure a good bond between the layers. The installation process is illustrated in Fig. 3.

Fig. 3. First and last layer of the installation process of GD.

After the successful installation in the mould, the surface was covered waterproof, and the beam was left to rest for a day at room temperature before being tested. If the beam had to be prepared for testing at higher temperatures in a climate chamber, it was stored, protected against desiccation, in an oven. Before installation in the testing machine, the beam was removed from the mould, measured and weighed.

4 Bending tests

4.1 Testing procedure

A beam-bending device, originally designed to investigate concrete beams, was used to perform the tests. To simulate realistic conditions in landfill sealings, the bearings and the loading device were modified compared to an initial study of this problem in [1]. Flat bearings replaced the two punctiform bearings, and the beams were loaded with a surface load. The load was applied by a hydraulic cylinder with a specified loading rate. A water-filled pressure pad was installed between the beam and the loading device to ensure an even load distribution. The applied load was then measured with tactile pressure matrix sensors

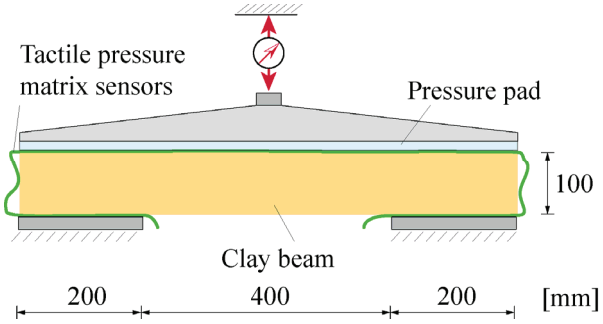

Fig. 4. Schematic illustration of the test setup [1].

during the test and stored for the subsequent analysis. A schematic illustration of the setup is shown in Fig. 4.

The beams were placed in the testing machine and equipped with up to four mini-tensiometers in the tensile areas to investigate the change in soil suction. During the test, the vertical force was measured via the oil pressure and the deflection at the centre of the beam with an inductive displacement transducer. Fig. 5 shows the test setup for a TK clay beam.

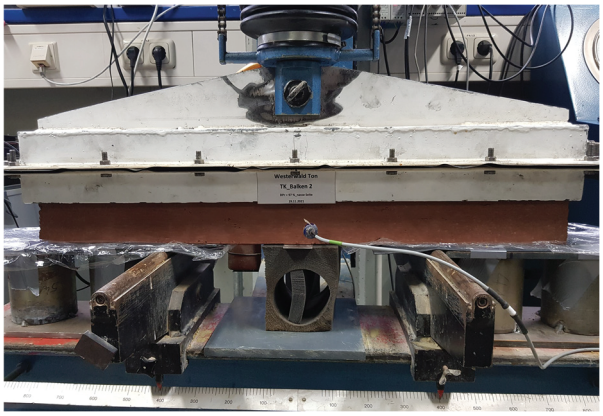

Fig. 5. TK clay beam with one tensiometer before testing.

To cover the entire length of the beams with tactile pressure matrix sensors, two foils were used, as shown in Fig. 6. The sensors were directly connected to a computer that recorded the pressure distribution over time. It was also possible to display the current pressure distribution graphically.

The bending tests in the climate chamber were carried out at a temperature of 55 °C and relative humidity of 30 %. The test setup displayed in Fig. 7 is essentially the same as that at room temperature, except that the tensiometers could not be used here because they would not have withstood the high temperature.

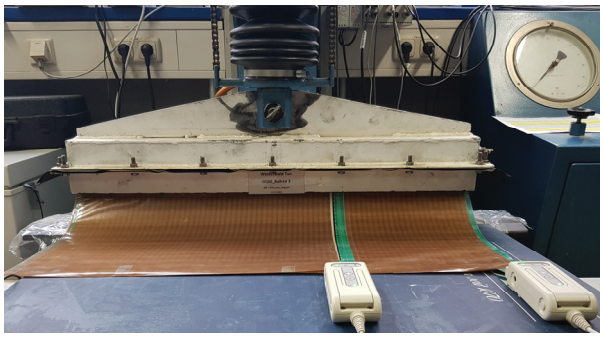

Fig. 6. Beam equipped with two pressure sensor foils.

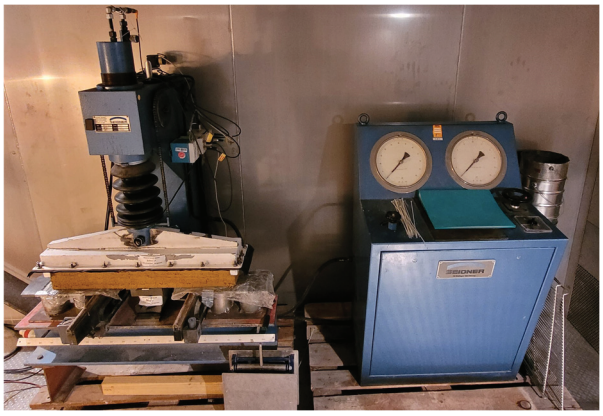

Fig. 7. Test setup inside the climate chamber.

All beams were loaded displacement-controlled up to failure with a low loading rate of approx. 0.5 mm/min and a high loading rate of approx. 2 mm/min. The load at which the first crack occurred in the beam and the corresponding deflection were stored for later evaluation. A GD beam at the end of a test is shown in Fig. 8.

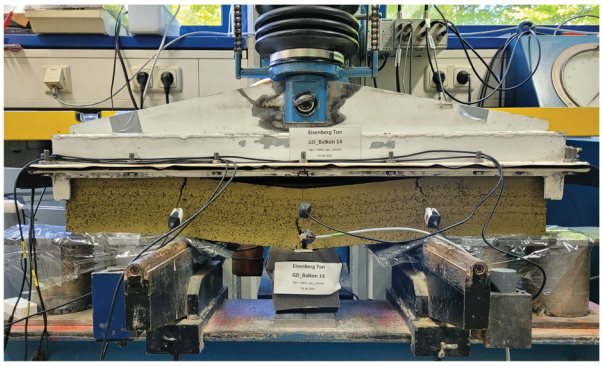

Fig. 8. GD clay beam loaded up to failure.

4.2 Test results

4.2.1 Pressure distribution

Fig. 9 shows the evolution of the pressure distribution over time for the beam GD_8.2. The marked area corresponds to the dimensions of the beam. The mean pressure over that area at selected time points during the test is also displayed in that figure. Pressure contours outside the marked area are due to the folding of the film and are therefore not relevant.

The white areas at the beginning of the test, cf. top plot in Fig. 9, indicate that the pressure pad partially touches the beam top surface. Nevertheless, it can already be seen from the shadings that the applied load is evenly distributed. With further increase of the load, cf. centre plot in Fig. 9, the pressure pad presses almost entirely the beam top surface and ensures a uniform load distribution. When the load reaches its maximum value and the first cracks occur in the beam, the desired uniform load distribution shown in the bottom part of Fig. 9 arises. Local stress peaks in the contour plots are due to imperfections of the beam surface related to the manual preparation and are irrelevant.

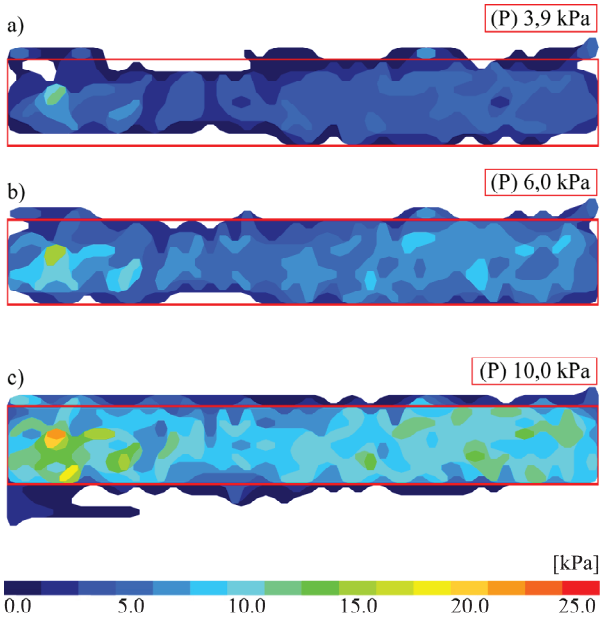

Fig. 9. Pressure distribution at the beginning (a), in the middle (b) and at the end of the bending test (c).

To verify the accuracy of both the loading cell and the tactile pressure sensors, the measured load at failure is divided by the top surface area of the beam and compared to the average pressure recorded by the sensors. These values are designated as p_{load} and p_{tact}, respectively, and are given in Table 3 for two typical tests, showing a good agreement between the two methods.

Table 3. Applied pressure on the top of the beam at failure as obtained from the load cell and the tactile sensors.

	p_{load} [kPa]	p_{tact} [kPa]
Beam GD_8.2	9.8	10.0
Beam TK_7	34.7	32.3

4.2.2 Bending tests at room temperature

The results of the GD test series at two loading rates are shown in Fig. 10, where failure is marked with a cross. For the tests at the lower rate, diagram (a), the maximum attainable load with the lowest deflection occurs for D_{Pr} = 97 % 'dry side' condition, whereas the maximum deflection is observed for D_{Pr} = 100 %. The smallest load is measured for the beam with D_{Pr} = 97 % 'wet side'. It can further be seen that the beams behave more ductile as water content increases.

The results of the tests at a higher loading rate, diagram (b) in Fig. 10, exhibit similar behaviour. Here, the maximum load and the lowest deflection occur for the beam with the lowest water content. As the water content increases, the deflection at failure also increases. For the beam with optimum water content D_{Pr} = 100 %, the higher loading rate yields a significantly higher load at failure and increases the associated deflection.

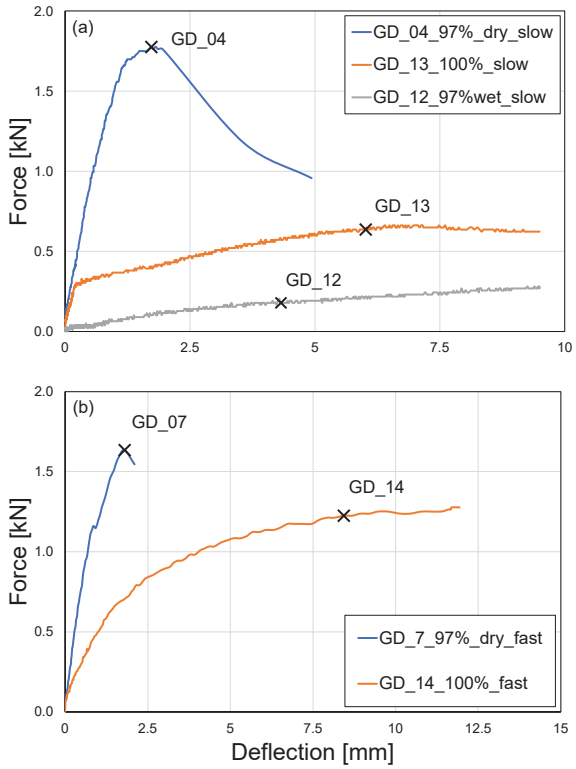

Fig. 10. Results of the GD beam series.

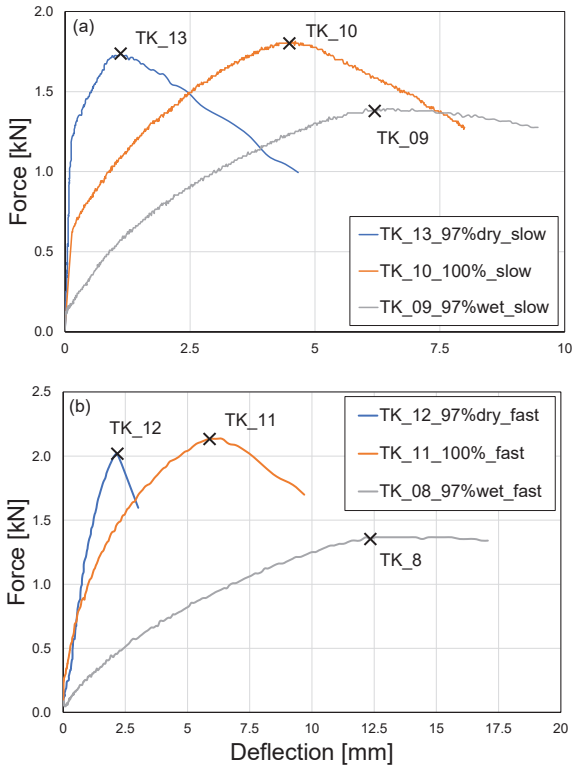

Fig. 11. Results of the TK beam series.

The results of the TK series at two loading rates are displayed in Fig. 11 and show a different bearing behaviour. At the lower loading rate, in diagram (a), the maximum load is observed for the beam with D_{Pr} = 100 %, while the largest deflection at failure occurs for the beam with D_{Pr} = 97 % 'wet side'. It can be seen that the load at failure first increases with increasing saturation up to the optimum water content and then

decreases, while the corresponding deflection increases with increasing water content.

Similar behaviour can also be seen in the tests with the higher loading rate, diagram (b) in Fig. 11. The higher rate leads to a significant increase in the attainable load and deflection at failure. As in the case of the GD clay, this test series also yields a more ductile behaviour as water content increases.

4.2.3 Bending tests inside the climate chamber

The same tests were carried out in a climate chamber at a constant temperature of 55 °C and a relative humidity of 30 %. However, only the tests with the low loading rate could be executed due to the limited availability.

The high temperature caused some of the beams with D_{Pr} = 97 % 'dry side' to dry out and collapse even before the tests started.

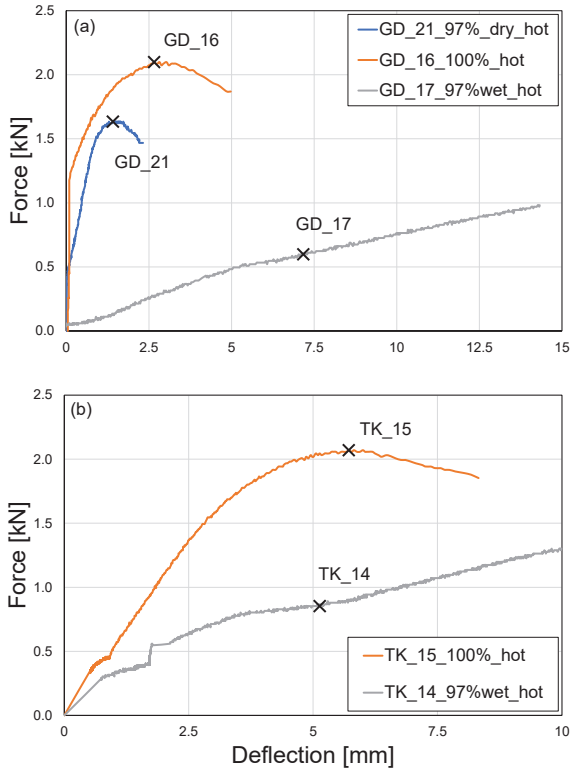

Fig. 12. Results of the GD series (a) and the TK series (b).

The results of the two test series are shown in Fig. 12. The GD clay tests show similarities and differences to those at room temperature. The highest load is observed for D_{Pr} = 100 %, and the lowest deflection for D_{Pr} = 97 % 'dry side'. As for room temperature conditions, the load at failure decreases with increasing water content, while the opposite is observed for the deflection at failure. A minor change is observed for D_{Pr} = 97 % 'dry side' compared to the test at room temperature. For D_{Pr} = 97 % 'wet side, the results show a significant increase in both the maximum load and deflection compared to the test at room temperature.

For the TK clay, cf. Fig. 12, the maximum load and deflection at failure occur for D_{Pr} = 100 %. The beam with D_{Pr} = 97 % 'wet side' shows a notably lower maximum load and deflection. Compared with the tests at room temperature, the beam with D_{Pr} = 100 % exhibits a slightly greater maximum load and deflection at failure. The results for D_{Pr} = 97 % 'wet side' differ from those at room temperature: both the maximum load and the corresponding deflection are lower, whereby the differences are more pronounced for the load at failure.

4.2.4 Matric suction measurement

To measure the matric suction during the test, selected beams were equipped with mini tensiometers, which were placed in pre-drilled holes before the start of the test. After the tensiometers indicated a constant matric suction, the test was started, and the beam was loaded until failure. No measurements could be taken on the beams with D_{Pr} = 97 % 'dry side' because the matric suction values were outside the range of the tensiometers.

Fig. 13 shows the results for a GD clay test with D_{Pr} = 100 % at low and high loading rates. In both cases, the matric suction increased continuously from the initial value to the value at failure. The comparatively highest load and deflection at failure occurred in the tests with a high loading rate. The different initial values of the matric suction for beams with the same water content result from the inhomogeneous water content distribution in the beams.

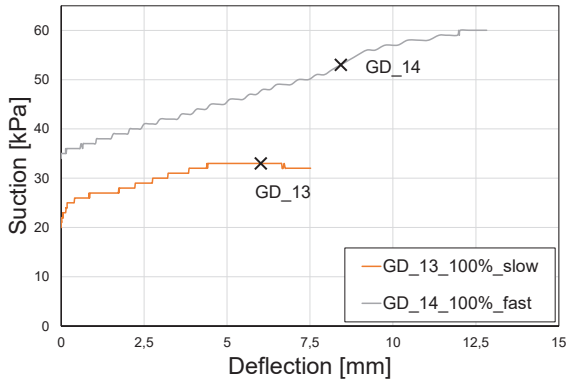

Fig. 13. Matric suction at different loading speeds.

5 Conclusions

To investigate the deformation behaviour of partially saturated clay beams under flexural stress, beams of two different clays were prepared and loaded to failure in bending tests. The beams were tested using a specially modified loading device in a bending machine. By employing tactile pressure matrix sensors, it was shown that this modified loading device ensures a constant load distribution on the beams.

The beams were prepared with three different degrees of saturation, and the bending tests were carried out with two different loading rates and at two different ambient temperatures. The tests at room temperature and 55 °C in the climate chamber clearly showed the influence of both the degree of saturation and the loading rate on the maximum load and deflection at failure. It has also been shown that the beams behave more ductile with increasing water content.

For selected beams, the matric suction in the tension zone was measured by employing mini-tensiometers. All tests showed that the matric stress increases continuously from its initial value to the value at failure.

The authors wish to thank the German Research Foundation DFG for the financial support of the project and the SIBELCO company for providing the clays.

References

1. C. Vrettos, A. Becker, *Bending tests on two clays and deformability verification for a multifunctional landfill liner* (in German), geotechnik **40** (4), pp. 232–241 (2017)
2. D.G. Fredlund, H. Rahardjo, *Soil mechanics for unsaturated soils* (2010)
3. R.M. Zeh, K.J. Witt, *The tensile strength of compacted clays as affected by suction and soil structure*, in Experimental Unsaturated Soil Mechanics, Springer Proc. in Physics **112**, pp. 219–226 (2007)
4. J. Köditz, R.-B. Wudtke, K.J. Witt, *Comparison of direct and indirect test methods for determining the tensile strength of cohesive soils* (in German), geotechnik **39** (4), pp. 225–234 (2016)
5. V. Dagar, E. Cokca, *A study on tensile strength of compacted fine-grained soils*, Geotech. Geol. Eng. **39** (2), pp. 751–764 (2021)
6. A. Ajaz, R.H.G. Parry, *Stress–strain behaviour of two compacted clays in tension and compression*, Géotechnique **25** (3), pp. 495–512 (1975)
7. A. Ammeri, M. Jamei, M. Bouassida, O. Ple, P. Villard, J.P. Gourc, *Numerical study of bending test on compacted clay by Discrete Element Method: tensile strength determination*, Int. J. Comput. Appl. T. **34** (1), pp. 13–22 (2009)
8. J.P. Gourc, S. Camp, B. Viswanadham, S. Rajesh, *Deformation behavior of clay cap barriers of hazardous waste containment systems: Full-scale and centrifuge tests*, Geotext. Geomembranes **28** (3), pp. 281–291 (2010)
9. N.I. Thusyanthan, W.A. Take, S.P.G. Madabhushi, M.D. Bolton, *Crack initiation in clay observed in beam bending*, Géotechnique **57** (7), pp. 581–594 (2007)
10. P. Schick, *Performance and evaluation of splitting tensile tests with cohesive soils* (in German), Bautechnik **82** (2), pp. 90–104 (2005)
11. A. Ajaz, R.H.G. Parry, *Analysis of bending stresses in soil beams*, Géotechnique **25** (3), pp. 586–591 (1975)